Impact of baryon resonances on the chiral phase transition at finite temperature and density

D. Zschiesche,[1] G. Zeeb,[1] S. Schramm,[1] and H. Stöcker[1,2]

[1]*Institut für Theoretische Physik, Robert-Mayer-Str. 8-10, D-60054 Frankfurt am Main, Germany*

[2]*Frankfurt Institute for Advanced Studies (FIAS), Robert-Mayer-Str. 10, 60054 Frankfurt am Main, Germany*

(Dated: October 31, 2005)

Abstract

We study the phase diagram of a generalized chiral SU(3)-flavor model in mean-field approximation. In particular, the influence of the baryon resonances, and their couplings to the scalar and vector fields, on the characteristics of the chiral phase transition as a function of temperature and baryon-chemical potential is investigated. Present and future finite-density lattice calculations might constrain the couplings of the fields to the baryons. The results are compared to recent lattice QCD calculations and it is shown that it is non-trivial to obtain, simultaneously, stable cold nuclear matter.

I. INTRODUCTION

QCD is the accepted underlying theory of strong interactions. It exhibits a very diverse and fascinating phase structure. At high temperatures or chemical potentials two different significant changes in the structure of matter are expected: Deconfinement [1] and chiral symmetry restoration [2, 3, 4]. Relativistic heavy ion collisions and astrophysical objects like neutron stars are two important experimental windows to gain information about these transitions, where extreme conditions of temperature and/or density occur. In the hadronic world, as well as in the region not too far above the phase transition to the deconfined and chirally restored phase, the strong coupling constant is large and thus QCD can not be treated perturbatively. From a theoretical point of view, lattice gauge calculations represent the most direct approach to investigate the QCD phase diagram of strongly interacting matter. In the last years many lattice results on the phase structure of QCD at finite temperature T and (recently) also at finite chemical potential μ were obtained (see e.g. [5, 6, 7, 8, 9, 10, 11, 12, 13, 14]). In particular, the properties of the chiral and deconfinement phase transitions and thermodynamic observables like pressure and energy density were investigated. However, lattice QCD alone does not seem to be able to completely disentangle the physics of the QCD phase transition and give an explanation of the structure and the scales of the phase diagram. Uncertainties in the lattice results remain, as e.g. the large pion mass, large lattice spacings, or the reliability of the expansion schemes and the continuum limit [14]. Furthermore, in order to understand the dynamics of relativistic heavy ion collisions and the structure of neutron stars, the equation of state of strongly interacting matter is needed also at very high μ. This is a region lattice QCD can not describe reliably up to now and probably neither in the near future. Thus, effective lagrangians [15, 16] are studied, representing a complementary approach to disentangle and understand the physics of the QCD phase transition (see e.g [2, 17, 18, 19, 20, 21, 22, 23, 24, 25, 26, 27, 28, 29, 30, 31] or Refs. in [32]).

At high temperatures, so-called hadron resonance models represent a very successful effective approach. The hadronic Bootstrap model [33] predicted the existence of a limiting temperature for hadronic matter long before lattice QCD provided first evidence for the transition to the deconfined, chirally restored phase [7]. Furthermore, for quark masses currently used in lattice calculations a resonance gas model with a percolation criterion

gives a reasonable description of lattice data close to T_c [7]. As was shown in [12, 13], the density dependence of the QCD equation of state in the hadronic phase observed in recent lattice studies can be understood in terms of a baryonic resonance gas. Finally, the critical temperature $T_c(\mu = 0)$ from lattice QCD depends only weakly on changes of the lightest hadron masses [7], in contrast to the predictions of a linear $SU(2) \times SU(2)$ linear σ model [17] without resonances. The pressure of heavy states, however, may reduce the dependence of T_c on the quark masses [34], in accord with the findings from the lattice. Furthermore, we point out that typically models relying mainly on order-parameter (infra-red) dynamics and which do not include more massive states predict significantly smaller phase transition temperatures in baryon-dense matter than obtained on the lattice (see e.g. Fig. 6 in [32]).

These findings indicate that a hadron resonance gas approach is reasonable below T_c and that in such an approach the contributions of heavy resonances are very important. Even though the free resonance gas gives a very good description of the lattice data – the same lattice data unambigiously show that there are temperature and medium effects, for example the change in the chiral condensate [7]. This is not accounted for in non-interacting approaches. In addition, studies of the nucleon-nucleon interaction and dense nuclear matter in boson exchange models show the importance of various meson exchanges [35]. Many properties of finite nuclei and of nuclear matter saturation can be understood in terms of scalar and vector potentials [36, 37, 38, 39].

Furthermore, it is desirable that effective models incorporate some known features of QCD. Thus, an interacting hadron gas accounting for chiral symmetry restoration and other known medium effects should be investigated, like it has been done e.g. in [23]. To this end, we consider here the phase transition properties of the chiral hadronic model presented in [40]. It represents a relativistic field theoretical model of baryons and mesons built on chiral $SU(3)_L \times SU(3)_R$ symmetry and broken scale invariance. A non-linear realization (see [41, 42]) of chiral symmetry is adopted. The model has been shown to successfully describe hadronic vacuum properties, nuclear matter saturation, finite nuclei and hypernuclei [40, 43, 44]. Furthermore, it has been applied to the description of hot and cold non-strange and strange hadronic matter [45], the structure of rotating neutron stars [46, 47] and observables in relativistic heavy ion collisions [48, 49]. In Refs. [49, 50] it was shown that a chiral phase transition to a chirally restored phase occurs at high densities or temperatures. At vanishing chemical potential the critical temperature is $150 - 180$ MeV, i.e. in the range

predicted by lattice calculations. The nature of this transition – at finite temperature as well as at finite chemical potential – crucially depends on the number of degrees of freedom coupled to the mesonic fields and on the strength of these couplings [49, 51, 52]. For a deeper understanding of the chiral phase transition in strongly interacting matter, we will thus systematically analyze the role of baryon resonances, which in our investigation are effectively represented by the lightest baryon decuplet.

Note that only the *chiral* transition is adressed by our model since only hadronic degrees of freedom are considered. Nevertheless, we can ask when particle densities are that large that hadrons should no longer be the suitable degrees of freedom anymore. It turns out that the coupling of the baryon decuplet may give the right scale for the critical temperature and also lead to a drastically increasing energy- and baryon density at the phase boundary. By simultaneously studying different observables, like here the predicted phase diagram and nuclear matter saturation, it is possible to relate these different aspects of strongly interacting matter. This should on one hand help to get a deeper understanding of the different regions of the QCD phase diagram and on the other hand provide more constraints on effective models, especially in the resonance sector but also, for example, on the form of the potentials. Furthermore, we can study how the restoration and the different symmetry breaking patterns are reflected in the properties of the model under different external conditions.

The paper is organized as follows. In section II we introduce the chiral SU(3) model. Section III shows the results for the phase diagram and for thermodynamic observables. In section IV we conclude and give an outlook to future work.

II. THE CHIRAL MODEL

The chiral hadronic SU(3) lagrangian in the mean field approximation has the following basic structure

$$\mathcal{L} = \mathcal{L}_{\rm kin} + \mathcal{L}_{\rm BM} + \mathcal{L}_{\rm BV} + \mathcal{L}_{\rm vec} + \mathcal{L}_0 + \mathcal{L}_{\rm SB} \ , \tag{1}$$

consisting of interaction terms between baryons respectively spin-0 (BM) and spin-1 (BV) mesons

$$\mathcal{L}_{\rm BM} + \mathcal{L}_{\rm BV} \ = \ -\sum_i \overline{\psi}_i \left[g_{i\sigma}\sigma + g_{i\zeta}\zeta + g_{i\omega}\gamma_0\omega^0 + g_{i\phi}\gamma_0\phi^0 \right] \psi_i \ ,$$

$$\mathcal{L}_{\rm vec} \;=\; \frac{1}{2}m_\omega^2\frac{\chi^2}{\chi_0^2}\omega^2 + \frac{1}{2}m_\phi^2\frac{\chi^2}{\chi_0^2}\phi^2 + g_4^4(\omega^4 + 2\phi^4) \tag{2}$$

summing over the baryonic octet (N,Λ,Σ,Ξ), and decuplet (Δ,Σ*,Ξ*,Ω). The interactions between the scalar mesons (with the scale breaking terms containing the dilaton field χ) read

$$\begin{aligned}\mathcal{L}_0 \;=\; & -\frac{1}{2}k_0\chi^2(\sigma^2+\zeta^2) + k_1(\sigma^2+\zeta^2)^2 + k_2(\frac{\sigma^4}{2}+\zeta^4) + k_3\chi\sigma^2\zeta \\ & - k_4\chi^4 - \frac{1}{4}\chi^4\ln\frac{\chi^4}{\chi_0^4} + \frac{\delta}{3}\ln\frac{\sigma^2\zeta}{\sigma_0^2\zeta_0}\;. \end{aligned} \tag{3}$$

An explicit symmetry breaking term mimics the QCD effect of non-zero current quark masses

$$\mathcal{L}_{\rm SB} \;=\; -\left(\frac{\chi}{\chi_0}\right)^2\left[m_\pi^2 f_\pi\sigma + (\sqrt{2}m_K^2 f_K - \frac{1}{\sqrt{2}}m_\pi^2 f_\pi)\zeta\right]\;. \tag{4}$$

The term $\mathcal{L}_{\rm kin}$ in (1) contains the kinetic energy terms of the hadrons. The general model incorporates the full lowest baryon (octet and decuplet) and meson multiplets. Here, instead, we only consider the mesons relevant for symmetric nuclear matter, namely the scalar field σ and its $s\bar{s}$ counterpart ζ (which can be identified with the observed f_0 particle), as well as the ω and ϕ vector mesons. All other mesons as well as heavier baryon resonances are treated as free particles and thus do not act as sources of the field equations. The term $\mathcal{L}_{\rm vec}$ generates the masses of the spin-1 mesons through the interactions with spin-0 mesons. The scalar interactions $\mathcal{L}_0$ induce the spontaneous chiral symmetry breaking. Another scalar isoscalar field, the dilaton χ, which simulates the breaking of the QCD scale invariance, can be identified with the gluon condensate [53] (for a more detailed discussion see [40]). The effective masses $m_i^*(\sigma,\zeta) = g_{i\sigma}\,\sigma + g_{i\zeta}\,\zeta$ of the baryons are generated through their coupling to the scalar fields, which attain non-zero vacuum expectation values due to the self-interactions [40] [62]. For the decuplet D we introduce an explicitly symmetry breaking mass term of the form

$$\mathcal{L} = -m_{\rm Dec}\bar{D}D\,. \tag{5}$$

With this term, it is possible to systematically study how the strength of the scalar coupling of the resonances influences the properties of hadronic matter, as will be discussed in more detail. In the strange sector an additional symmetry breaking term of the form $m_3(\sqrt{2}(\sigma-\sigma_0)+(\zeta-\zeta_0))$ is introduced, where $m_3 = 1.25$. It is chosen in accord with the octet sector [40, 49], and guarantees that the decuplet masses always stay above the corresponding octet masses [63].

The resulting mass terms read

$$\begin{aligned}
m_\Delta &= m_{\rm Dec} + g_D^S \left[(3-\alpha_{DS})\sigma + \alpha_{DS}\sqrt{2}\zeta\right] \\
m_{\Sigma^*} &= m_{\rm Dec} + m_3(\sqrt{2}(\sigma-\sigma_0)+\zeta-\zeta_0) + g_D^S \left[2\sigma + \sqrt{2}\zeta\right] \\
m_{\Xi^*} &= m_{\rm Dec} + m_3(\sqrt{2}(\sigma-\sigma_0)+\zeta-\zeta_0) + g_D^S \left[(1+\alpha_{DS})\sigma + (2-\alpha_{DS})\sqrt{2}\zeta\right] \\
m_\Omega &= m_{\rm Dec} + m_3(\sqrt{2}(\sigma-\sigma_0)+\zeta-\zeta_0) + g_D^S \left[2\alpha_{DS}\sigma + (3-\alpha_{DS})\sqrt{2}\zeta\right] \ . \qquad (6)
\end{aligned}$$

The two extreme cases $m_{\rm Dec} = 0$ and $m_{\rm Dec} = 1232$ MeV correspond to the parameter studies CII and CI in Ref. [49], respectively [64].

For a given value of the explicit symmetry breaking $m_{\rm Dec}$, the two couplings g_D^S and α_{DS} are adjusted to the vacuum masses of the decuplet resonances. (Note that the coupling of the Δ to the strange condensate is non-zero but small.)

The vector couplings $g_{i\omega}$ and $g_{i\phi}$ for the octet as well as for the decuplet result from pure f-type coupling as discussed in [40, 54],

$$\begin{aligned}
g_{i\omega} &= (n_q^i - n_{\bar{q}}^i) g_{8,10}^V \\
g_{i\phi} &= -(n_s^i - n_{\bar{s}}^i)\sqrt{2} g_{8,10}^V \, , \qquad (7)
\end{aligned}$$

with $i = N, \Lambda, \Sigma, \Xi, \Delta, \Sigma^*, \Xi^*, \Omega$, while g_8^V and g_{10}^V denote the vector coupling of the baryon octet and decuplet, respectively. n^i represents the number of constituent quarks of a particular species in a given hadron, where the index q represents the light u- and d-quarks, s the strange quark, and $\bar{q}, \bar{s}$ the corresponding antiquarks. The resulting relative couplings correspond to the additive quark model constraints.

The grand canonical thermodynamic potential of the system can be written as

$$\frac{\Omega}{V} = -\mathcal{L}_{\rm vec} - \mathcal{L}_0 - \mathcal{L}_{\rm SB} - \mathcal{V}_{\rm vac} \mp T \sum_i \frac{\gamma_i}{(2\pi)^3} \int d^3k \left[\ln\left(1 \pm e^{-\frac{1}{T}[E_i^*(k) - \mu_i^*]}\right)\right] , \qquad (8)$$

where γ_i denote the hadronic spin-isospin degeneracy factors and $E_i^*(k) = \sqrt{k_i^2 + m_i^{*2}}$ are the single particle energies. The effective chemical potentials read $\mu_i^* = \mu_i - g_{i\omega}\omega - g_{i\phi}\phi$, with $\mu_i = (n_q^i - n_{\bar{q}}^i)\mu_q + (n_s^i - n_{\bar{s}}^i)\mu_s$. The vacuum energy $\mathcal{V}_{\rm vac}$ (the potential at $\rho_B = T = 0$) has been subtracted in order to get a vanishing vacuum energy.

By extremizing Ω/V one obtains self-consistent equations for the meson fields. We here consider non-strange matter, i.e., for given T- and μ_q-values the strange chemical potential

μ_s is chosen such that the net number of strange quarks in the system is zero. Then the dominant fields are the σ and the ω. Their field equations read

$$\begin{aligned}
\frac{\partial(\mathcal{L}_0)}{\partial\sigma} + \frac{\partial(\mathcal{L}_{\rm SB})}{\partial\sigma} &= \sum_i \frac{\partial m_i^*}{\partial\sigma}\frac{\gamma_i}{(2\pi)^3}\int d^3k \frac{m_i^*}{E_i^*}\left(n_{k,i}+\bar{n}_{k,i}\right) \equiv \sum_i g_{i\sigma}\rho_i^s \\
\frac{\chi}{\chi_0}\, m_\omega^2\omega + 4g_4^4\omega^3 &= \sum_i g_{i\omega}\frac{\gamma_i}{(2\pi)^3}\int d^3k \left(n_{k,i}-\bar{n}_{k,i}\right) \equiv \sum_i g_{i\omega}\rho_i,
\end{aligned} \tag{9}$$

with the fermionic (anti-)particle distribution functions

$$n_{k,i} \equiv n_{k,i}(T,\mu_i^*) = \frac{1}{e^{\frac{1}{T}[E_i^*-\mu_i^*]}+1} \tag{10}$$

$$\bar{n}_{k,i} \equiv \bar{n}_{k,i}(T,\mu_i^*) = \frac{1}{e^{\frac{1}{T}[E_i^*+\mu_i^*]}+1}, \tag{11}$$

while ρ_i^s and ρ_i denote the scalar and vector density of particle species i, respectively.

The sources for the scalar and vector fields mainly depend on two parameters: the number of degrees of freedom coupled to the fields and the corresponding coupling constants. For the octet, the scalar couplings are fixed by the vacuum masses and the vector coupling is adjusted to give the correct binding energy of nuclear matter [40].

In the current investigation we will systematically study the dependence of the hadronic matter properties on the strength of the scalar and vector coupling for the decuplet. These are controlled by the explicit symmetry breaking $m_{\rm Dec}$ and the relative strength of the vector coupling,

$$r_{\rm v} = \frac{g_{10}^V}{g_8^V} = \frac{g_{\Delta\omega}}{g_{N\omega}}, \tag{12}$$

respectively [65]. The two parameters $m_{\rm Dec}$ and $r_{\rm v}$ determine the abundance and the contribution of the baryon resonances to the scalar and vector field equations and, as will be shown later, also determine the phase diagram of the model. From Eq. (6) one sees that the larger the explicit symmetry breaking value $m_{\rm Dec}$, the smaller are the resulting decuplet-scalar couplings $g_{i\sigma}$, $g_{i\zeta}$, i.e. the contribution of the resonances to the source terms of the field equations. In addition, a large explicit symmetry breaking $m_{\rm Dec}$ also gives a higher effective mass in the medium. Equation (12) shows that the larger $r_{\rm v}$, the larger is g_{10}^V, which leads to smaller effective potentials μ_i^* for the decuplet states. This reduces the net number of baryon resonances at a given chemical potential.

III. RESULTS

First, we concentrate on the phase transition behavior at vanishing chemical potential. Since the vector field ω couples to the vector densities ρ_i, it vanishes independently of the coupling chosen. Thus, the phase transition behavior at $\mu = 0$ depends only on the scalar coupling, i.e. on the choice of $m_{\rm Dec}$, not on $r_{\rm v}$. Figure 1 shows the scalar fields σ and ζ as a function of temperature T for different values of the scalar coupling. For $m_{\rm Dec} < 260$ MeV (i.e. $g_{\Delta\sigma} \gtrsim g_{N\sigma}$), a first-order phase transition occurs, as indicated by the jump in the chiral condensates at $T_c \approx 155$ MeV. For smaller couplings of the baryon resonances the scalar fields decrease continuously and a crossover is observed. The strange condensate ζ is much less affected around T_c than the non-strange condensate σ, reflecting the fact that most of the produced pairs are nucleons and deltas. If the value of the additional symmetry breaking for the strange resonances (m_3 from Eq. 6) is decreased – re-adjusting the corresponding coupling strength to keep the masses at their vaccuum expectation values – these decuplet states contribute stronger and might even produce another first-order phase transition characterized by a discontinuity in the strange condensate. This will be discussed in detail in [55].

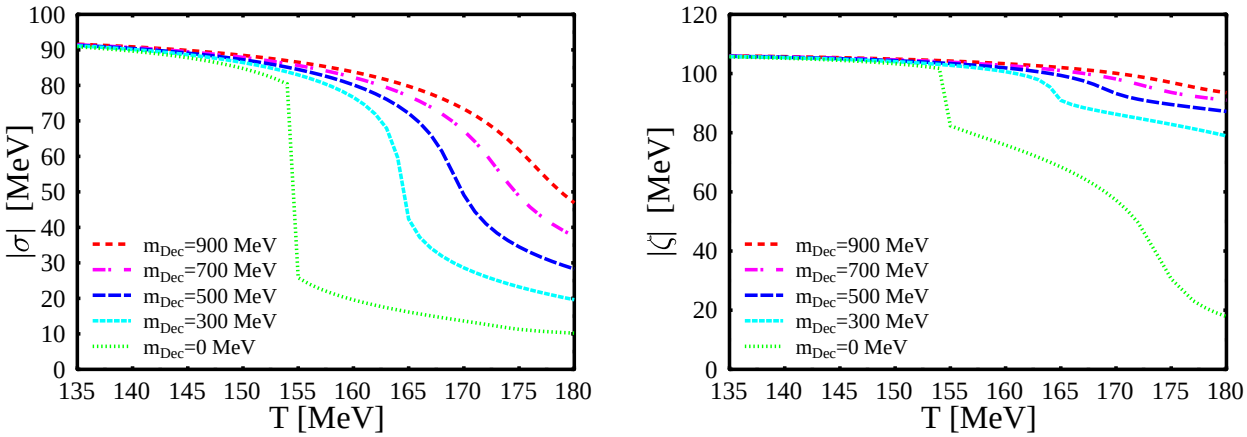

FIG. 1: Non-strange condensate σ (left) and strange condensate ζ (right) as a function of temperature for vanishing chemical potential (μ_q=0). The curves correspond to different values of the explicit symmetry breaking term $m_{\rm Dec}$.

For given T- and μ_q-values the thermodynamic potential is given by Eq. (8). Minima in the potential characterize the different phases present. In addition, the knowledge of the

potential as a function of the fields, i.e. away from the minimum, is also of interest, e.g. for non-equlibrium dynamics of the phase transition [56]. In Fig. 2 the effective potential for two different values of the scalar coupling of the baryon resonances is depicted around T_c. For $m_{\rm Dec} = 0$ (left) two distinct minima appear, showing the same depth at T_c (full line). Thus, at this temperature the stable phase of the system jumps from large to low σ values. For $m_{\rm Dec} = 300$ MeV, in contrast, there exists only one minimum in the effective potential which continuously changes with temperature. This characterizes the crossover transition.

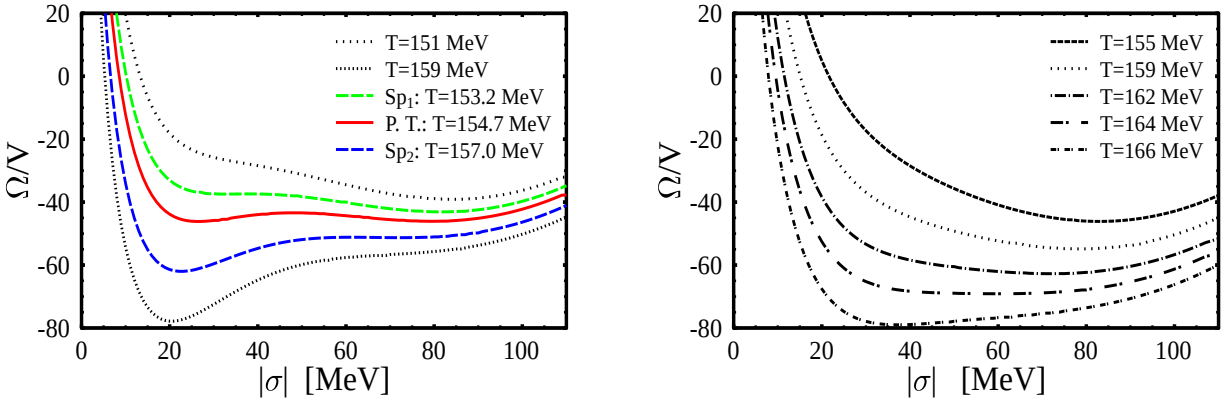

FIG. 2: Effective potential as a function of (the order parameter) σ. The left panel depicts the case with a first-order phase transition for $m_{\rm Dec} = 0$. In between both of the spinodals (broken lines) the potential has two minima which have the same depth at the phase transition temperature (full line). The right panel shows an example for the crossover case, here $m_{\rm Dec} = 300$ MeV. The minimum of the potential achieves values of the σ-field of ≈ 20 MeV yet at notably higher temperatures than in the first-order phase transition case.

We now turn to finite chemical potentials to investigate the phase diagram in the whole T-μ plane. Recent lattice QCD data predict a crossover at vanishing chemical potential [5, 14, 57] and a critical end point at $T_c \approx 150 - 170$ MeV and $\mu_{q,c} \approx 100 - 250$ MeV. Since several sources of uncertainty remain in these calculations, as e.g. the large π mass or the finite lattice spacings, we will also discuss the case of a first-order phase transition at $\mu = 0$. First, however, we want to consider the case with a crossover at $\mu = 0$. As discussed above this is obtained for $m_{\rm Dec} \geq 260$ MeV. Then, the highest T_c is obtained for a minimal vector coupling $r_{\rm v} = 0$. We find $T_c \approx 155$ MeV and $\mu_{q,c} \approx 70$ MeV. The resulting phase diagram is depicted in Fig. 3 (left), showing a critical point in the same region as predicted by lattice

QCD. However, the critical temperature drops much faster in our model calculation than in the lattice results. Increasing the vector coupling of the baryon resonances decreases T_c and increases $\mu_{q,c}$ (see Fig. 3 middle and right). Very similar behavior is observed when decreasing the scalar coupling and keeping the vector coupling constant. However, for all choices shown in Fig. 3 ($r_{\rm v} = 0, 0.2, 0.4$), the chiral phase transition occurs at $\mu_q < 300$ MeV for $T = 0$, which implies a stable chirally restored phase. Hence, the current form of the model it is not able to obtain simultaneously a critical temperature in the region predicted by lattice QCD and a successful description of nuclear matter properties (density, binding energy).

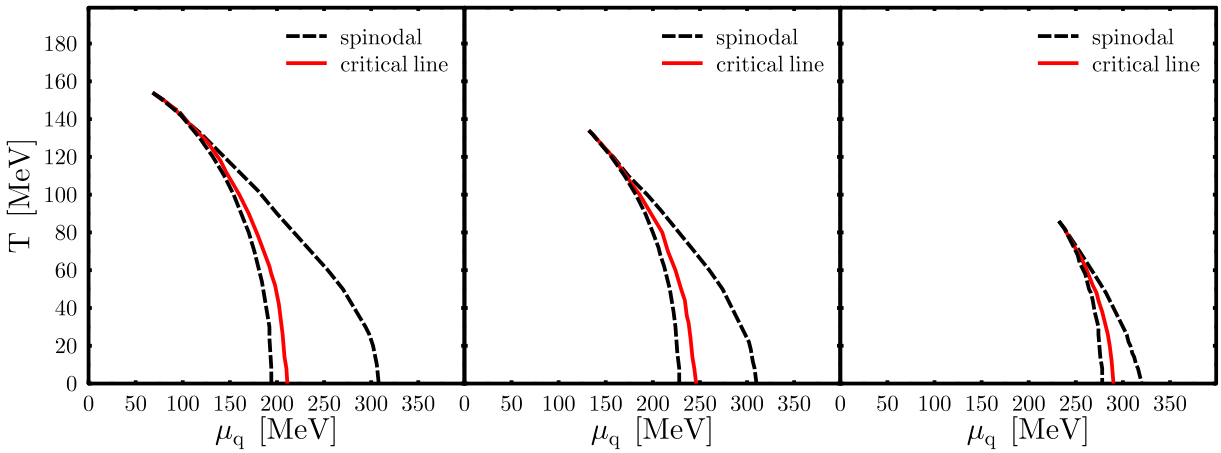

FIG. 3: Phase diagram for $m_{\rm Dec} = 300$ MeV and increasing values of the decuplet vector coupling from left to right ($r_{\rm v} = 0, 0.2, 0.4$).

In Fig. 4 (left) we show the parameter regions, which, at $T = 0$, either give a first-order phase transition and an absolutely stable chirally restored phase, or a chiral phase transition but stable normal nuclear matter, or no phase transition at all (crossover), respectively. We observe that the smaller the explicit symmetry breaking term $m_{\rm Dec}$, i.e. the larger the scalar coupling of the baryon resonances, the larger the vector coupling constant must be chosen to guarantee stable normal nuclear matter. This is in agreement with the results obtained in [45, 52, 58]. Insisting that normal nuclear matter be stable reduces the maximum critical temperature to $T_c \approx 50$ MeV, with a critical chemical potential $\mu_{q,c} \approx 290$ MeV. This phase diagram is shown in Fig. 4 (right) for $m_{\rm Dec} = 300$ MeV and $r_{\rm v} = 0.5$, the correspondingly

lowest possible value for $r_{\rm v}$, which leads to stable normal nuclear matter. The resulting phase diagrams for higher values of the explicit symmetry breaking $m_{\rm Dec}$ and the corresponding smallest possible vector couplings, look nearly identical. Thus, in the present form the chiral model yields $T_c \lesssim 50$ MeV, if we insist on normal nuclear matter being stable.

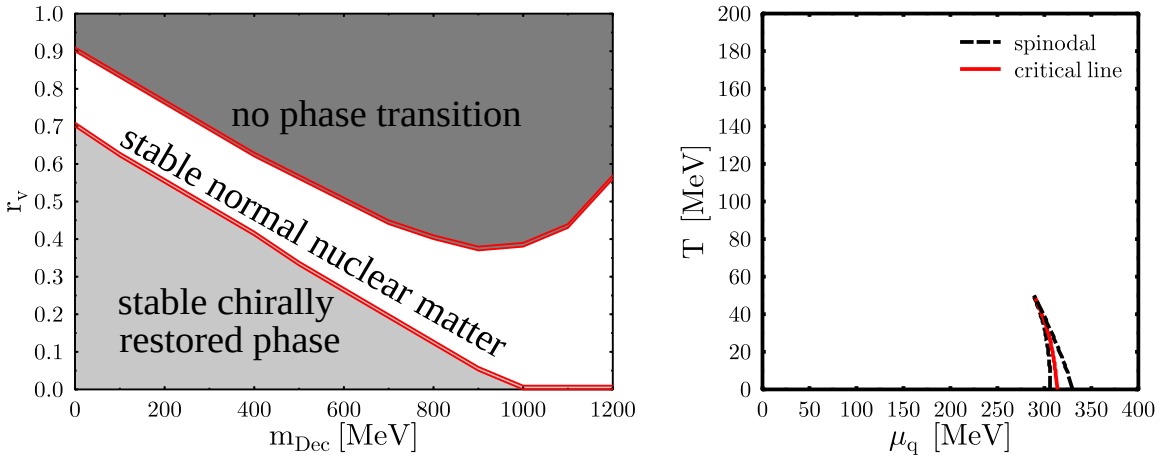

FIG. 4: (Left) Regions in the $r_{\rm v}$–$m_{\rm Dec}$ parameter space giving a first-order phase transition with an absolutely stable chirally restored phase, a chiral phase transition but stable normal nuclear matter and a crossover, respectively, for $T = 0$. (Right) Phase diagram for $r_{\rm v}$ and $m_{\rm Dek}$ chosen such that nuclear matter is stable ($m_{\rm Dek} = 300$ MeV and $r_{\rm v} = 0.5$).

Examples for the energy density are shown in Fig. 5 as a function of temperature at constant chemical potential and for different values of $r_{\rm v}$ and $m_{\rm Dec}$ (broken lines) as well as for an ideal hadron gas (full lines). The left panel shows the case for $\mu_q = 0$, where $r_{\rm v}$ has no influence due to the vanishing net baryon density. The right panel shows the case for $\mu_q = 170$ MeV, illustrating the qualitatively similar effect of increasing either $r_{\rm v}$ or $m_{\rm Dec}$. For both chemical potentials the interacting and the free gas show similar properties at low T, but exhibit large differences at higher T. For a first-order phase transition the energy density jumps to extremely high values (dashed line on right panel).

Recent lattice QCD results show a crossover at $\mu = 0$. However, as stated above, several uncertainties remain. Thus, we also want to consider a first-order phase transition at $\mu = 0$. Then, new and different structures can be observed as shown in Fig. 6 for $m_{\rm Dec} = 0$. The

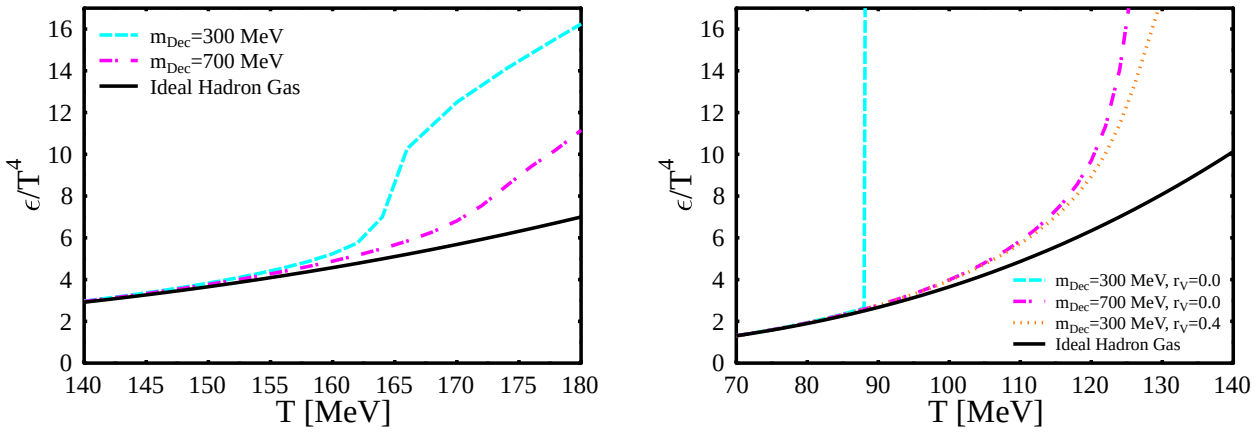

FIG. 5: Energy density over T^4 as a function of T with $\mu_q = 0$ (left) and $\mu_q = 170$ MeV (right) for different values of $r_{\rm v}$ (for $\mu_q \neq 0$) and $m_{\rm Dec}$. In each figure, one can clearly see the rapid departure of the model results from the ideal hadron gas curve (full line) in the respective phase transition region.

line representing the first-order phase transition starts from the T-axis. For small $r_{\rm v}$ this line continues down to the μ_q-axis. However, the phase transition weakens at moderate chemical potential, then becomes stronger again as $T \to 0$. For $r_{\rm v} \gtrsim 0.5$ the first-order phase transition line ends at $\mu_q \approx 100$ MeV and re-appears again at high chemical potentials if $r_{\rm v} \leq 0.9$ (cf. Fig. 4 left).

The right panel shows the prediction for an acceptable description of nuclear matter groundstate properties. The first-order phase transition line starting from $\mu = 0$ ends in a critical point $T_c \approx 150$ MeV and $\mu_{q,c} \approx 100$ MeV. For 150 MeV $\leq \mu_q \leq$ 280 MeV a crossover occurs. Then a first-order phase transition line appears again, reaching down to the $T = 0$ axis. This phase diagram differs markedly from the lattice results. Figure 7 shows how this behavior is reflected in the non-strange condensate. One can clearly see the jumps in the σ-field for low and high chemical potentials and the continuous behavior for intermediate μ_q. The phase transition at high temperatures and small chemical potentials is driven by the abundant production of particle-antiparticle pairs, which decreases the chiral condensates and thus the effective baryon masses. Therefrom a further increase of the pair production results. This is a similar mechanism as the one described in [51]. At small temperatures and high chemical potentials the phase transition is driven by the rapid increase of the vector density of the baryon resonances, especially the Δs, leading to a second minimum in the

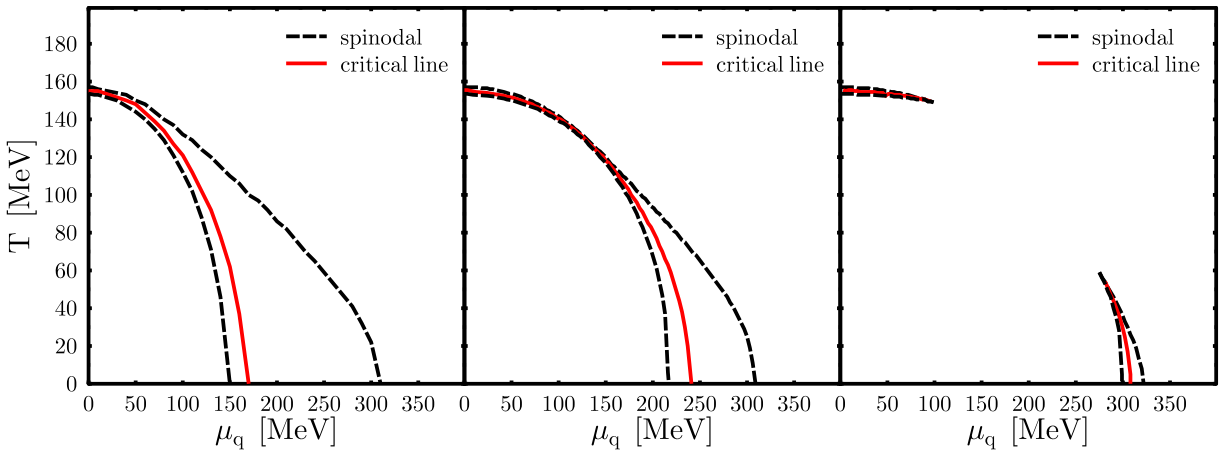

FIG. 6: Phase diagram for $m_{\rm Dec} = 0$ and $r_{\rm v} = 0, 0.4, 0.7$ (from left to right). For $r_{\rm v} = 0.4$ the phase transition weakens at intermediate chemical potentials and for $r_{\rm v} \geq 0.5$ the phase transition line is disconnected, as can be seen in the right figure for $r_{\rm v} = 0.7$, which yields stable nuclear matter.

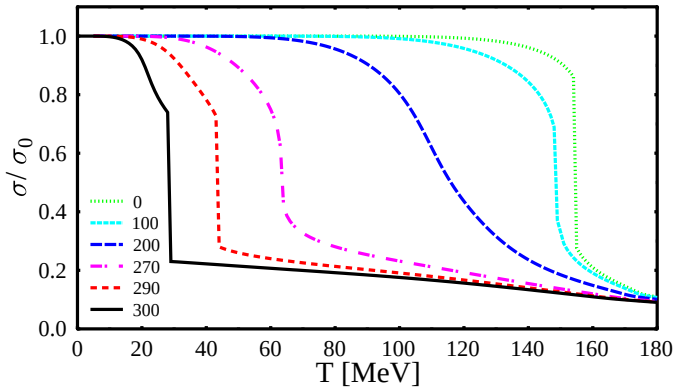

FIG. 7: Non-strange condensate σ as a function of temperature for $m_{\rm Dec} = 0$, $r_{\rm v} = 0.7$ and for different values of the chemical potential $\mu_q = 0 \ldots 300$ MeV. For low and high chemical potential the σ-field jumps, which corresponds to a first-order phase transition. For intermediate values of μ_q, instead, a continuous behavior results.

energy per particle.

IV. CONCLUSION

Using a chiral $SU(3)$ model we investigated the dependence of the QCD phase diagram on the scalar- and vector-coupling of the baryon decuplet. We found that qualitative agreement

with recent lattice results can be obtained, as for example a critical point around $T_c \approx 150$ MeV and finite $\mu_{q,c}$. However, the slow decrease of the phase transition temperature with increasing chemical potential could not be reproduced. Moreover, demanding existence of a normal nuclear matter ground-state at $T = 0$ reduces T_c significantly to approximately 50 MeV. Allowing for a first-order phase transition at $\mu = 0$, which cannot unambigiously be excluded from current lattice data, a rich phase structure is possible, depending on the vector coupling of the baryon resonances. If these are chosen to be small then a continuous first-order phase transition line from the T- to the μ-axis results. However, if the vector coupling is increased, the first-order phase transition line starting at the T-axis ends at intermediate chemical potentials. Depending on the adopted vector coupling, a first-order phase transition line re-appears at higher chemical potentials and lower temperature. Hence, there are two critical endpoints appearing in the QCD phase diagram for such a choice of parameters.

These results show that the simultaneous description of the phase diagram and nuclear matter saturation gives strong constraints on the model. Even more constraints may appear if also neutron stars are considered [59]. Since many different models with different equations of state give a good description of nuclear matter saturation and neutron stars, such additional constraints are urgently needed – although there is still considerable uncertainty in the lattice calculations. However, further improvement can be expected in the near future in this area and thus more reliable results will appear. Then one should be able to find connections between the phase diagram and the structure of specific models.

Our results also show that a very diverse structure of the phase diagram is possible. To get a better understanding of the characteristics of the phase transition at high chemical potential, it would be very helpful to gain knowledge on the latent heat and correlation lengths as a function of chemical potential from lattice calculations. Then one might be able to pin down the phase diagram in a more quantitative fashion.

Although our study neglected many contributions, especially the pions and the higher resonances, some very interesting conclusions appear. First of all, the baryon resonances may very well drive the chiral phase transition and give a structure in agreement with lattice QCD. The question how the QCD phase diagram with realistic pion masses looks like is still open. As was shown in [32], several different approaches, which do not take into account baryon resonances, yield much lower critical temperatures. This clearly suggests

an important role of baryonic degrees of freedom for the characteristics of the chiral phase transition. The stronger curvature of $T_c(\mu)$ as compared to lattice results might be due to only including the baryon decuplet. At the same time, however, the validity of a hadronic description of the thermodynamic state becomes quite questionable due to the 'explosion' of density and energy density at the first-order chiral phase transition.

So far we only took into account the contribution of the resonances by coupling the baryon decuplet to the fields. The extension to more degrees of freedom is in progress. It will be very interesting to see how the results obtained here may be changed by a larger hadronic spectrum.

Another very promising investigation is the comparison to the equation of state and the chiral condensate as obtained from lattice calculations with a distorted mass spectrum – as proposed in [12, 13]. There it was shown that a non-interacting resonance gas can give a good description of the lattice equation of state. Since close to T_c the effect of interactions should definitely be present, however, the comparisons to the lattice results should help to disentangle the field contributions from those of an ideal gas and to learn more about the nature of the interactions close to the phase boundary. In particular, within the chiral $SU(3)$ model one is able to study the behavior of the chiral condensate and thermodynamic quantities simultaneously. In addition, it is possible to make contact between the theory of the phase diagram and experimental observables, e.g. by determining in one model the chemical freeze-out temperature in relativistic heavy ion collisions – as obtained from fits to the measured particle ratios – and the phase transition temperature [60, 61].

The authors are grateful to Adrian Dumitru, Carsten Greiner, Jürgen Schaffner-Bielich, and Kristof Redlich for fruitful discussions. This work is supported by Deutsche Forschungsgemeinschaft (DFG), Gesellschaft für Schwerionenforschung (GSI) and Bundesministerium für Bildung und Forschung (BMBF). This work used computational resources provided by the Center for Scientific Computing (CSC) at the University of Frankfurt, Germany.

[1] B. Svetitsky and L.G. Yaffe, Nucl. Phys. B210 (1982) 423.

[2] D.A. Kirzhnits and A.D. Linde, Phys. Lett. B42 (1972) 471.

[3] Y. Nambu and G. Jona-Lasinio, Phys. Rev. 122 (1961) 345.

[4] S. Weinberg, Phys. Rev. D9 (1974) 3357.

[5] Z. Fodor and S.D. Katz, (2004), hep-lat/0402006.

[6] Z. Fodor and S.D. Katz, Phys. Lett. B534 (2002) 87, hep-lat/0104001.

[7] F. Karsch and E. Laermann, (2003), hep-lat/0305025.

[8] Z. Fodor, S.D. Katz and K.K. Szabo, Phys. Lett. B568 (2003) 73, hep-lat/0208078.

[9] F. Karsch et al., Nucl. Phys. Proc. Suppl. 129 (2004) 614, hep-lat/0309116.

[10] F. Karsch, K. Redlich and A. Tawfik, Phys. Lett. B571 (2003) 67, hep-ph/0306208.

[11] F. Karsch, (2004), hep-lat/0401031.

[12] F. Karsch, K. Redlich and A. Tawfik, Eur. Phys. J. C29 (2003) 549, hep-ph/0303108.

[13] F. Karsch, K. Redlich and A. Tawfik, Phys. Lett. B571 (2003) 67, hep-ph/0306208.

[14] P. de Forcrand and O. Philipsen, Nucl. Phys. B642 (2002) 290, hep-lat/0205016.

[15] S. Weinberg, Phys. Rev. Lett. 18 (1967) 188.

[16] S.R. Coleman, J. Wess and B. Zumino, Phys. Rev. 177 (1969) 2239.

[17] A. Dumitru, D. Roder and J. Ruppert, submitted to PRD (2003), hep-ph/0311119.

[18] T.D. Lee and G.C. Wick, Phys. Rev. D9 (1974) 2291.

[19] G. Baym and G. Grinstein, Phys. Rev. D15 (1977) 2897.

[20] R.D. Pisarski and F. Wilczek, Phys. Rev. D29 (1984) 338.

[21] B.A. Campbell, J.R. Ellis and K.A. Olive, Phys. Lett. B235 (1990) 325.

[22] B.A. Campbell, J.R. Ellis and K.A. Olive, Nucl. Phys. B345 (1990) 57.

[23] J.R. Ellis and K.A. Olive, Phys. Lett. B260 (1991) 173.

[24] G.E. Brown and M. Rho, Phys. Rev. Lett. 66 (1991) 2720.

[25] A. Patkos, Nucl. Phys. B365 (1991) 243.

[26] K. Kusaka and W. Weise, Phys. Lett. B288 (1992) 6.

[27] P.J. Ellis, E.K. Heide and S. Rudaz, Phys. Lett. B282 (1992) 271.

[28] K. Kusaka, W. Weise and M.K. Volkov, Phys. Lett. B302 (1993) 145.

[29] J. Schaffner-Bielich, Phys. Rev. Lett. 84 (2000) 3261, hep-ph/9906361.

[30] O. Scavenius et al., Phys. Rev. C64 (2001) 045202, nucl-th/0007030.

[31] D. Roder, J. Ruppert and D.H. Rischke, Phys. Rev. D68 (2003) 016003, nucl-th/0301085.

[32] M.A. Stephanov, (2004), hep-ph/0402115.

[33] R. Hagedorn, Nuovo Cim. Suppl. 3 (1965) 147.

[34] P. Gerber and H. Leutwyler, Nucl. Phys. B321 (1989) 387.

[35] R. Machleidt, ANP 19 (1989) 189.

[36] J.D. Walecka, Ann. Phys. (N.Y.) 83 (1974) 49.

[37] M.R. Anastasio et al., Phys. Rept. 100 (1983) 327.

[38] H. Duerr, Phys. Rev. 103 (1956) 469.

[39] B.C. Clark et al., Phys. Rev. C7 (1973) 466.

[40] P. Papazoglou et al., Phys. Rev. C 59 (1999) 411.

[41] S. Weinberg, Phys. Rev. Lett. 166 (1968) 1568.

[42] C.G. Callan et al., Phys. Rev. 177 (1969) 2247.

[43] S. Schramm, Phys. Rev. C66 (2002) 064310, nucl-th/0207060.

[44] C. Beckmann et al., Phys. Rev. C65 (2002) 024301, nucl-th/0106014.

[45] D. Zschiesche et al., Phys. Rev. C63 (2001) 025211, nucl-th/0001055.

[46] S. Schramm and D. Zschiesche, J. Phys. G29 (2003) 531, nucl-th/0204075.

[47] S. Schramm, Phys. Lett. B560 (2003) 164, nucl-th/0210053.

[48] D. Zschiesche et al., Phys. Lett. B547 (2002) 7, nucl-th/0209022.

[49] D. Zschiesche et al., Phys. Rev. C65 (2002) 064902, nucl-th/0107037.

[50] D. Zschiesche et al., Nucl. Phys. A663 (2000) 737, nucl-th/9908072.

[51] J. Theis et al., Phys. Rev. D 28 (1983) 2286.

[52] B.M. Waldhauser et al., Phys. Rev. C36 (1987) 1019.

[53] J. Schechter, Phys. Rev. D 21 (1980) 3393.

[54] D. Zschiesche et al., Springer Tracts in Modern Physics 163 (2000) 129.

[55] G. Zeeb et al., 2004, in preparation.

[56] K. Paech, H. Stocker and A. Dumitru, Phys. Rev. C68 (2003) 044907, nucl-th/0302013.

[57] F. Karsch, (2004), hep-lat/0403016.

[58] D. Kosov et al., PL B 421 (1998) 37.

[59] D. Zschiesche et al., J. Phys. G30 (2004) S381.

[60] D. Zschiesche et al., Phys. Lett. B547 (2002) 7, nucl-th/0209022.

[61] D. Zschiesche et al., J. Phys. G30 (2004) S381.

[62] For example in [23] the quark-hadron phase transition was investigated in an effective lagrangian approach only containing broken scale invariance. In this work we keep the gluon condensate frozen and thus focus on the role of the quark condensates. In a future work the case with a dynamical dilaton field will be addressed.

[63] To discuss the phase diagram, different symmetry breaking terms in the strange sector would have been possible. However, by choosing the same term as in former work we could make contact to the parameter studies made there. The difference to choosing an explicit symmetry breaking of the form $m_3 n_s(\sqrt{2}(\sigma - \sigma_0) + (\zeta - \zeta_0))$ is very small.

[64] As already shown in [49], the strength of the m_3-coupling also influences the phase structure of the model. In particular, two distinct phase transitions – corresponding to seperate discontinuities in the non-strange and the strange condensate – may occur. This will be discussed in detail in a future work, but here we will focus on the general role of the baryon resonances and thus only consider one way of explicit symmetry breaking.

[65] The decuplet couplings are partially constrained by the condition that nuclear matter and not the chirally restored phase is stable [45, 52, 58]. However, since we want to focus here on the general influence of the baryon resonances on the phase transition, they are treated as free parameters but it is always stated whether nuclear matter is stable or not.